NASA

Technical Memorandum 83865

An Optical Model for the Microwave Properties of Sea Ice

P. Gloersen and J.K. Larabee

NOVEMBER 1981

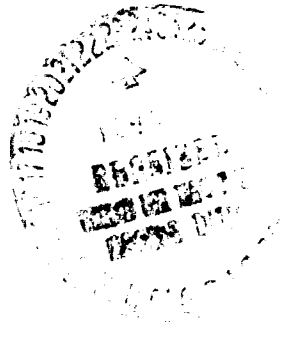

National Aeronautics and
Space Administration

Goddard Space Flight Center
Greenbelt, Maryland 20771

AN OPTICAL MODEL FOR THE MICROWAVE PROPERTIES OF SEA ICE

P. Gloersen and J. K. Larabee

NASA/GODDARD SPACE FLIGHT CENTER
Greenbelt, Maryland 20771

ABSTRACT

The complex refractive index of sea ice is modeled and used to predict the microwave signatures of various sea ice types. Results are shown to correspond well with the observed values of the complex index inferred from dielectric constant and dielectric loss measurements performed in the field, and with observed microwave signatures of sea ice. The success of this modeling procedure *vis* a *vis* modeling of the dielectric properties of sea ice constituents used earlier by several others is explained. Multiple layer radiative transfer calculations are used to predict the microwave properties of first-year sea ice with and without snow, and multiyear sea ice.

AN OPTICAL MODEL FOR THE MICROWAVE PROPERTIES OF SEA ICE

1. INTRODUCTION

There have been a number of earlier efforts to model the observed microwave properties of sea ice by use of mixing formulae combining the dielectric properties of the various constituents of the ice (Hoekstra and Capillino, 1971; Hallikainen, 1973; Vant, 1976). These efforts concentrated on modeling the complex dielectric constant of sea ice. Ice and water exhibit to first order a Debye relaxation spectrum, but the addition of dissolved salts introduces significant complexity. Results, therefore, were limited in range and required the use of adjustable parameters.

In this paper, we model the complex refractive index of sea ice. Results from the model correspond remarkably well with those inferred from dielectric constant and dielectric loss measurements performed in the field by Vant and others (1974). The attractive features of this alternate approach are (1) the mixing formula works equally well for both the real and imaginary parts of the index, and (2) no adjustable parameters are required. The success of linearly mixing the optical properties instead of the dielectric properties of sea ice constituents is in part explained by the nonlinear relationship between the complex refractive index and the complex dielectric constant.

Lastly, we discuss some multiple layer radiative transfer calculations to provide explanations for observed differences in the microwave properties of thin first-year sea ice without snow cover (FT), first-year sea ice with snow cover (FY), and multiyear sea ice (MY).

*Current address: Center for Earth and Planetary Physics, Harvard University, Cambridge, Massachusetts, 02138 USA

2. BASIC THEORY

If the variation of the electromagnetic fields in a conductor in space and time is expressed as $\exp(i\mathbf{k}\cdot\mathbf{r} - i\omega t)$, the complex index of refraction of the conductive medium is related to the wave number k of the disturbance by

$$k = \frac{2\pi}{\lambda} (n' + in'') \tag{1}$$

where n' and n'' denote the real and imaginary parts of the index, respectively, and λ is the wavelength *in vacuo* of the propagating plane wave. The power absorption coefficient β of the medium is therefore

$$\beta = \frac{4\pi n''}{\lambda} \tag{2}$$

i.e., the intensity of the wave is damped to e^{-1} of its initial value in a distance β^{-1}.

Application of the usual boundary conditions yields the Fresnel formalism for the relative complex amplitude of a reflected wave

$$\text{for H:} \quad \frac{E_{ref}}{E_{inc}} = \frac{n_1 \cos\theta - (n_2^2 - n_1^2 \sin^2\theta)^{1/2}}{n_1 \cos\theta + (n_2^2 - n_1^2 \sin^2\theta)^{1/2}} \tag{3a}$$

$$\text{for V:} \quad \frac{E_{ref}}{E_{inc}} = \frac{n_2^2 \cos\theta - n_1 (n_2^2 - n_1^2 \sin^2\theta)^{1/2}}{n_2^2 \cos\theta + n_1 (n_2^2 - n_1^2 \sin^2\theta)^{1/2}} \tag{3b}$$

where n_1 is the refractive index of the medium containing the incident wave, n_2 is the refractive index of the reflecting material, and θ is the angle of incidence (Jackson, 1975: p. 279 ff.). H and V refer to the polarization.

The reflectivity of an interface is defined as the ratio of the reflected energy flux to the incident energy flux, and is thus equal to the square of (3a) or (3b).

Thermodynamics requires the emissivity of a material to be related to the reflectivity via

$$e = 1 - R \tag{4}$$

Thermal radiation from an isotropic, homogeneous, flat half-space of ice in thermodynamic equilibrium at 250 K has a maximum of intensity at 11μm. Hence, at microwave wavelengths (0.1 - 100 cm) the Rayleigh-Jeans approximation to the Planck radiation law is valid, and it is standard to speak of radiances as brightness temperatures. Simple radiative transfer theory (Chandrasekhar, 1960; p. 13) yields in the case of one dimension

$$T_B = e \int_0^\infty T(z) \exp(-\tau(z)/\mu)\, d(\tau(z)/\mu) \tag{5}$$

where μ is the cosine of the angle of incidence and we have tacitly assumed that neither the physical temperature profile T nor the optical depth τ have any spatial dependence other than with the depth z. The optical depth is defined as

$$\tau(z) = \int_0^z \beta(z')\, dz' \tag{6}$$

where in general β is a function of several parameters of the medium.

For physical systems of interest, the upper limit of the integral in (5) is not infinite, but is a finite value τ_0/μ corresponding to a finite thickness Z_0 of the ice. The finitude of Z_0 admits the possibility of other contributions to the brightness temperature from underlying layers, with the appropriate depth scale dependent upon τ. Complications arise when the refractive index varies significantly over a "skin depth" ($1/\beta$). We will address these complications at a later stage.

3. FIRST-YEAR THIN (FT) ICE

Sea ice is a complex heterogeneous mixture of solid ice, air, precipitated salts, and brine. The brine component is localized within a system of brine cells, interconnected by drainage canals

(Untersteiner, 1968; Meeks and others, 1974). In response to temperature gradients, the brine cells diffuse to the warmer side (Hoekstra and others, 1965), rendering sea ice salinity profiles time dependent. Brine cells vary considerably in physical dimension and orientation with respect to the surface. In FT ice, the cells are approximately spherical and have a diameter on the order of a few millimeters (Ramseier and others, 1975). The brine itself is a complex solution of metal salts, predominantly NaCl, $MgCl_2$, and Na_2SO_4. The presence of these salts allows a small amount of liquid brine to remain in the ice down to temperatures as low as 230°K (Assur, 1958).

To the extent to which one can neglect scattering losses at microwave wavelengths, one can idealize FT ice for radiometric purposes as a vertically structured medium containing a volume fraction V_b of brine, a volume fraction V_a of air, and a remaining fraction $(1 - V_b - V_a)$ of pure ice. We hypothesize that the refractive index of FT ice may be modeled by linearly mixing the optical properties of the three constituents

$$n^i_{FT} = (1 - V_b - V_a)\, n^i_{ice} + V_b\, n^i_{brine} + V_a\, n^i_{air} \qquad (7)$$

where the superscript i signifies either n' or n''.

Knowledge of various components of equation (7) varies considerably. The behavior of the refractive index of pure ice (n^i_{ice}) with decreasing temperature is fairly well known (Figure 1). Interstitial air can be assumed to have the optical properties of vacuum. An adequate description of the refractive index of sea water however, (n^i_{brine}) at microwave wavelengths has proven elusive, despite the efforts of several researchers (Stogryn, 1971; Ho and Hall, 1973; Klein and Swift, 1977). In particular, results applicable to the salinities and temperatures encountered in sea ice brine cells are absent from the literature. Work by Lane and Saxton (1952a, 1952b) suggests that the optical properties of supercooled brines may vary in a continuous manner from the

better known optical properties of sea water at more elevated temperatures, though this hypothesis is as yet unsubstantiated.

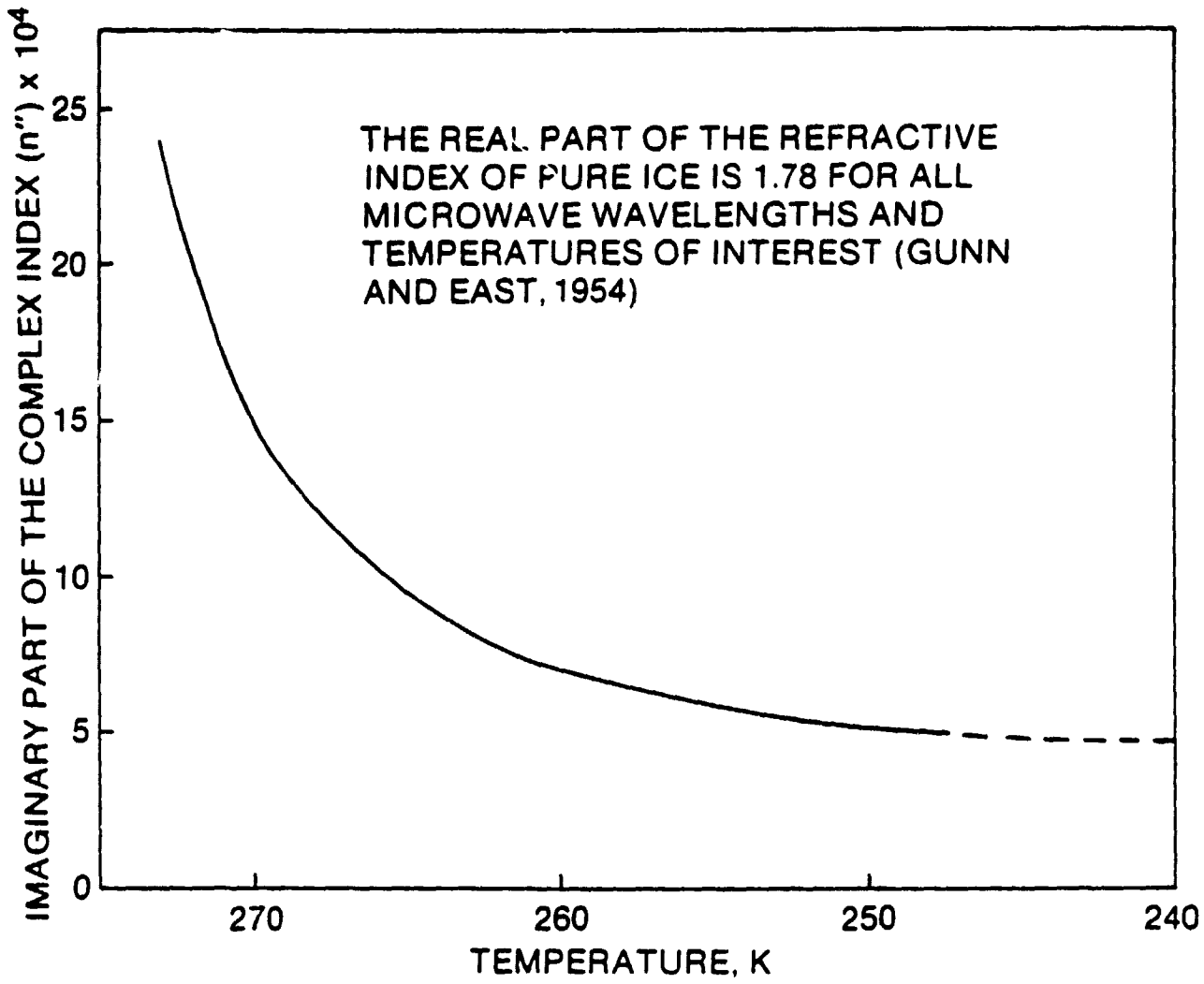

Figure 1. Real and imaginary parts of the complex index of refraction for pure ice.

Precipitated salts are known to comprise at most 1% of the ice volume (Meeks and others, 1974), which implies

$$V_a = 1 - (\rho_s/\rho_i). \qquad (8)$$

where ρ_s is the density of the ice sample and ρ_i is the density of pure ice. (0.917 g cm^{-3})

The brine volume fraction V_b as a function of temperature and salinity has been investigated by Assur (1958) and parameterized by Frankenstein and Garner (1967) and Poe et al. (1972), and is shown graphically in Figure 2.

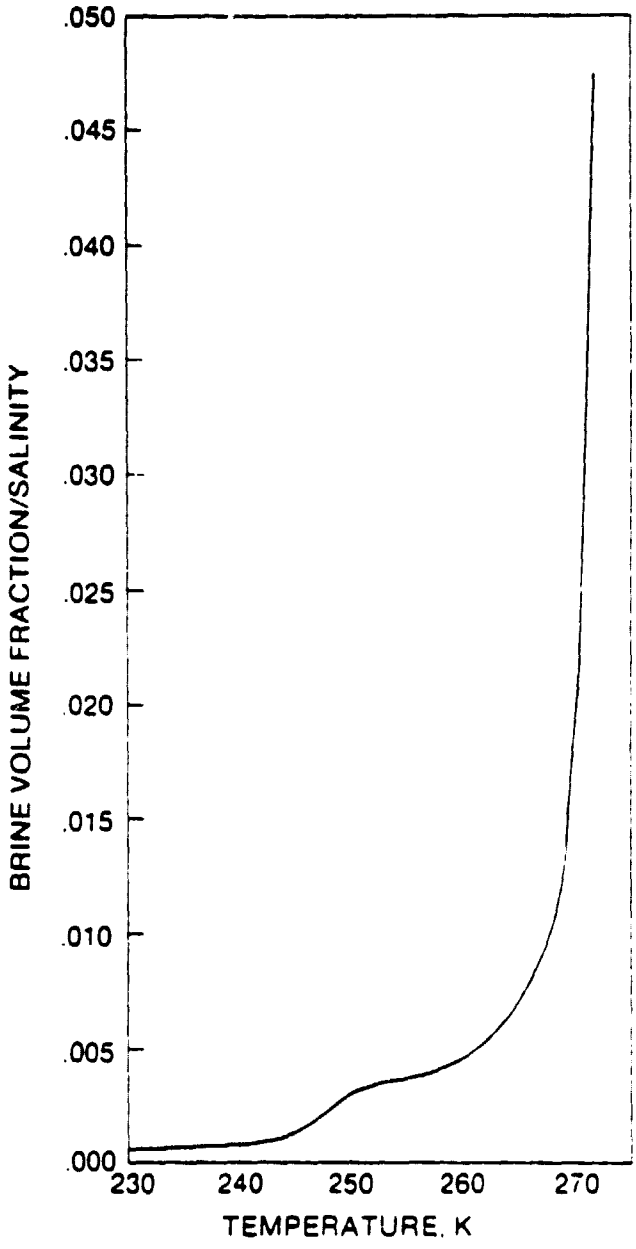

Figure 2. Ratio of the brine volume fraction to its salinity as a function of the ice temperature.

For a first order calculation, we have assumed that the optical properties of brine can be approximated by those of sea water. To simulate ambient ice conditions, we evaluate these properties at the freezing point of sea water (~ 271°K), using the equations of Klein and Swift (1977). The salinity value substituted into Klein and Swift's equations was the (field derived) average salinity of the ice. With these assumptions, model calculations for the refractive index of FT ice at 3.0 cm wavelength are shown in Figures 3 and 4. The data of Vant and others (1974) are plotted for comparison.

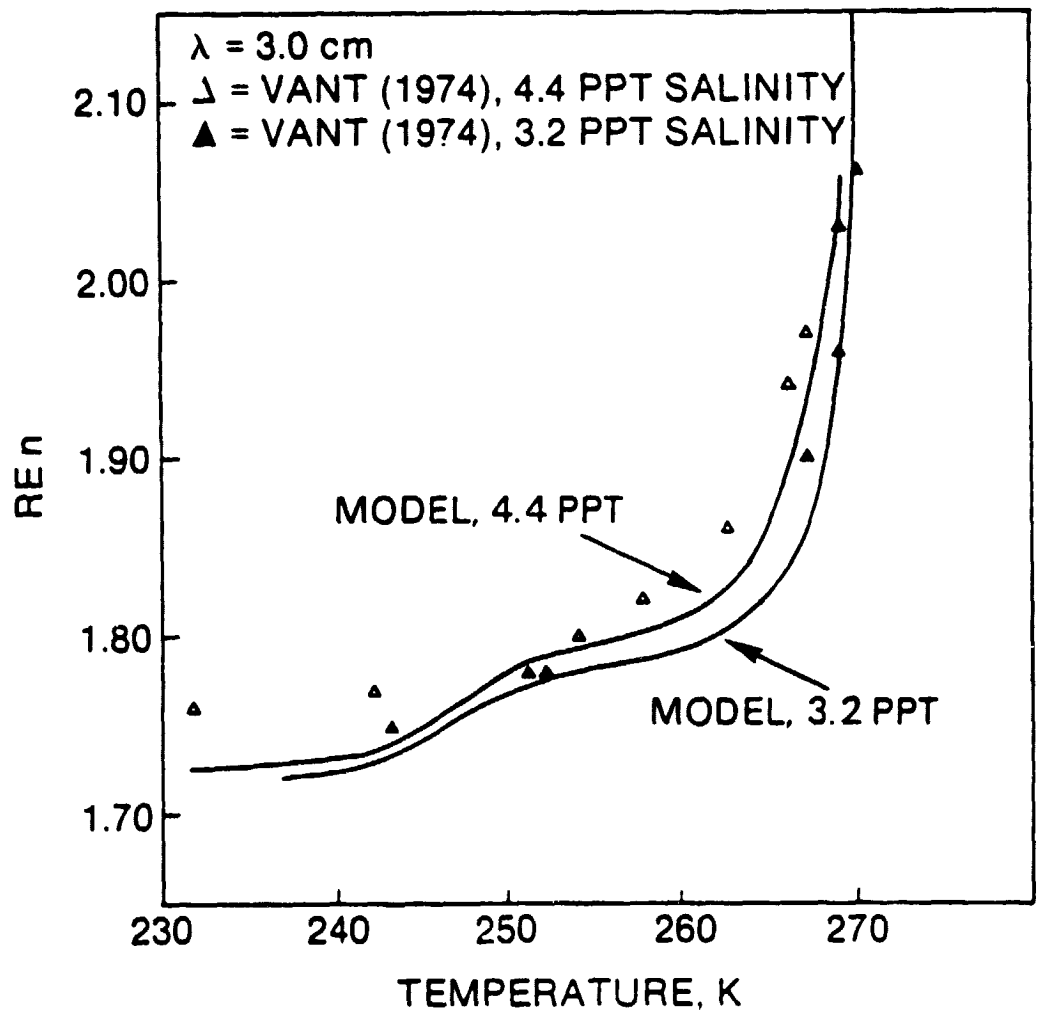

Figure 3. Comparison of the experimental values for the real part of the complex index of refraction for sea ice, obtained from data of Vant et al., and predicted values from the model presented here.

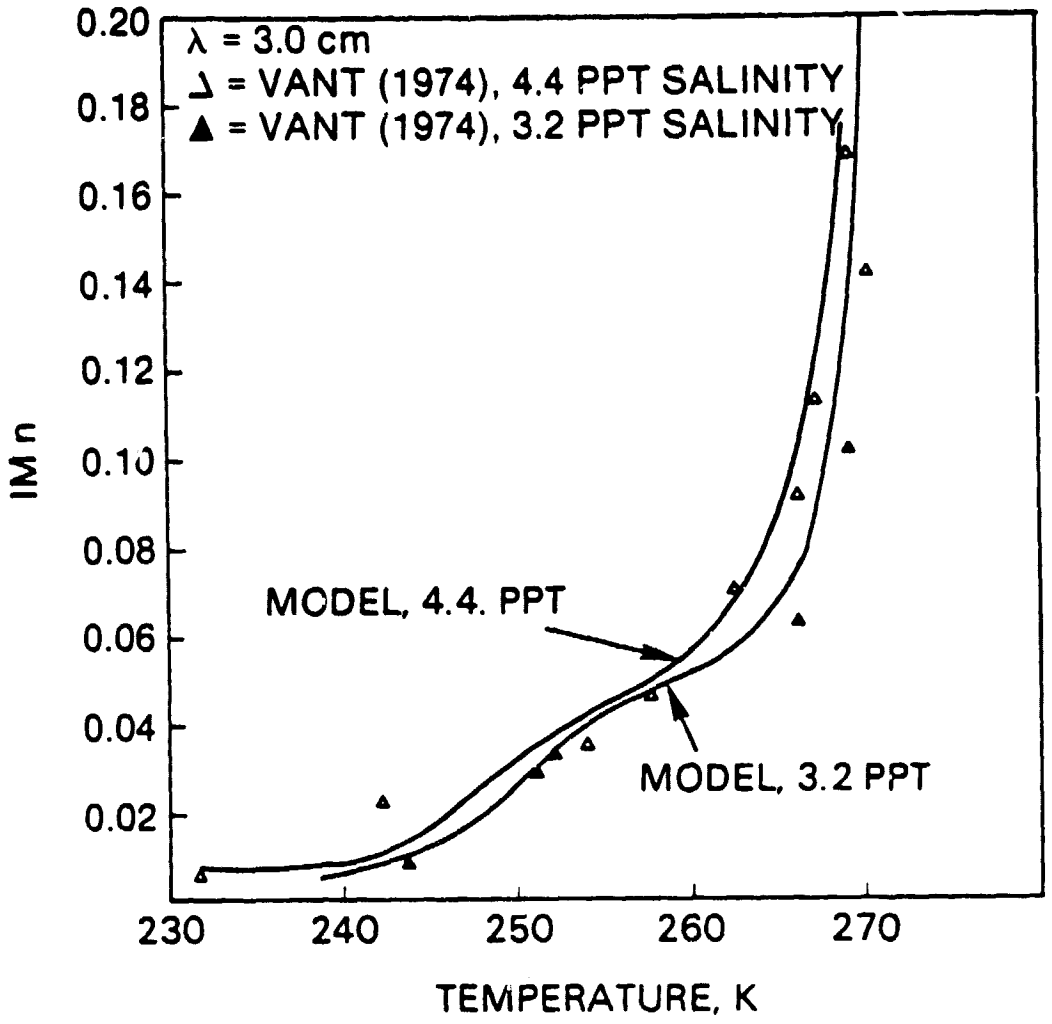

Figure 4. Comparison of the experimental values for the imaginary part of the complex index of refraction for sea ice, obtained from data of Vant et al., and predicted values from the model presented here.

The agreement between the linear mixing model and experimental data is quite good, differing only at very low temperatures (where extrapolations are probably least valid) and possibly near melting.

The FT ice dielectric data of Vant were collected by placing an ice sample in a waveguide and measuring the complex transmission coefficient of the sample. Numerical techniques were

employed to obtain the dielectric constant and loss tangent. For thin floating ice remotely sensed by airborne or spaceborne radiometers, however, thermal emission from underlying sea water contributes to the observed brightness temperature. We may operationally define "thin" ice as ice of thickness less than ten optical depths. Lake and river ice (low salinity) is virtually always thin ice, becoming opaque at thicknesses of the order of a hundred wavelengths. Young sea ice, principally because of its brine content, may be optically thick at tenths to tens of wavelengths.

The presence of two nearly parallel reflecting interfaces raises the possibility of interference phenomena contributing to observed brightness temperatures. Tiuri and others (1978) observed interference effects at wavelengths between 30 and 60 cm when acquiring data from helicopter-borne radiometers viewing low salinity FT ice in the Gulf of Bothnia. Basharinov and others (1974) reported interference beats when viewing Caspian Sea ice. Interference effects have been seen (Blinn, personal communication; Ramseier, personal communication) when measuring flowing river ice with *in situ* radiometers. These phenomena were not observed by airborne radiometers (Gloersen and others, unpublished data), presumably because thickness variations within an instantaneous field of view (IFOV) are sufficient to average out interference phenomena. This conclusion is supported by two observations: Blinn's data, acquired with a small IFOV, displayed more oscillations in brightness temperature as the ice thickness increased than did the data of Ramseier obtained with a larger IFOV.

Neglecting multiple reflection and interference effects, we may express the brightness temperature of FT thin ice by a radiative transfer equation of the form

$$T_B = \epsilon_1 \epsilon_2 T_{water} \exp(-\tau/\mu) + \epsilon_1 \Gamma_1 + \epsilon_1 (1 - \epsilon_2) T_2 \exp(-\tau/\mu) \qquad (9)$$

where the subscripts 1 and 2 refer to the ice/air and water/ice interfaces, respectively, and T_1 and

T_2 are effective temperatures described shortly. The first term on the right-hand side of (9) is the radiation emanating from the water attenuated by a (purely absorptive) pass through the ice layer and reflected at both interfaces, the second term is the upwelling radiation from the ice, and the last term is the downwelling radiation from the ice reflected upward and attenuated. The factor μ is related to the cosine of the incidence angle through Snell's law. Model geometry is shown in Figure 5.

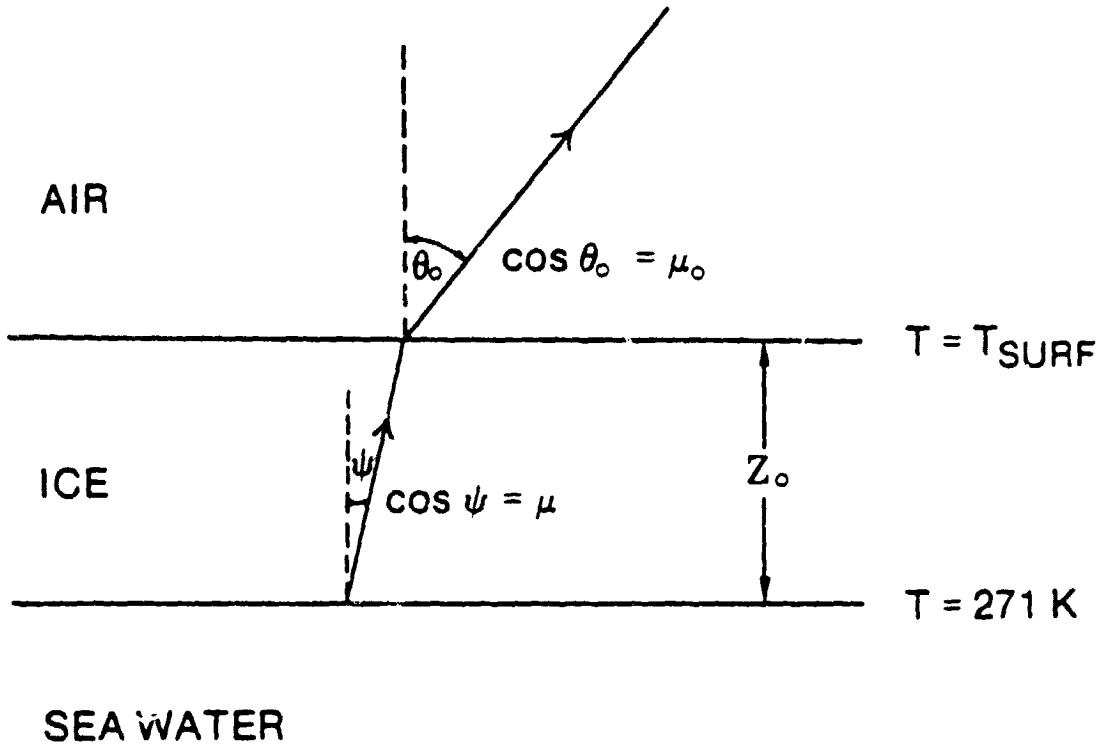

Figure 5. Model Schematic for thin sea ice.

The temperatures T_1 and T_2 are physical temperature profiles weighted by radiative transfer properties:

$$T_1 = \int_0^{\tau/\mu} T(z) \exp(-\tau'(z)/\mu)\, d(\tau'(z)/\mu) \qquad (10)$$

$$T_2 = \int_0^{\tau/\mu} T(z) \exp\left((-\tau + \tau'(z))/\mu \right) d(\tau'(z)/\mu) \qquad (11)$$

where T(z) is the physical temperature profile. Under steady-state conditions, this profile is linear (Chandrasekhar, 1960: p. 13).

$$T(z) = T_{surf} + z((T_{wat} - T_{surf})/Z_0) = T_{surf} + \delta \cdot z \qquad (12)$$

where T_{surf} is the physical temperature at the surface of the ice, T_{wat} is 271° K, and Z_0 is the thickness of the ice in centimeters. The depth dependence of the optical depth τ is given by (6); $\beta(z)$ has the functional form

$$\beta(z) = \alpha + \frac{\beta}{\gamma - \delta \cdot z} \qquad (13)$$

where

$$\alpha = \frac{.01257\ S}{\lambda}\ n'_{brine}$$

$$\beta = 44\alpha \qquad (°K\ cm^{-1})$$

$$\gamma = 273.15 - T_{surf} \qquad (°K)$$

$$\delta = (271 - T_{surf})/Z_0 \qquad (°K\ cm^{-1})$$

and S is the average salinity of the ice, measured in parts per thousand. This parameterization of the absorption coefficient is based on Figure 2 (for 250° K < T_{surf} < 270° K) and our mixing model.

Unfortunately, there are added complexities. Sea ice is neither an excellent conductor nor a good dielectric. We have also restricted ourselves in the present case to optically thin layers of ice. Hence, we are in an intermediary regime where neither geometrical nor physical optics is valid in a strict sense. The Fresnel formulae assumed that the thickness d of the transition layer

between the two media is small relative to λ. This transition layer thickness d is a measure of the inhomogeneities of the medium; if microscopic descriptions of the field are valid, the condition $d \ll \lambda$ is usually fulfilled. For $d \gg \lambda$, propagation of electromagnetic waves can be regarded as propagation of rays which are refracted in the transition layer but are not reflected (cf. Landau and Lifschitz, 1975; p. 272). The methods of variational calculus allow the generalization of Snell's law to a situation where the (complex) index of refraction varies continuously throughout a medium, but it is not clear such methods are valid when the refractive index varies by a large amount over thickness d.

We have chosen to restrict our analysis of FT ice in the following manner. We note the complexity of brightness temperatures observed by Tiuri and co-workers (1978) in the brackish waters of the Gulf of Bothnia and confine our attention, therefore, to relatively high salinity (3 ppt $< S <$ 10 ppt) FT ice. When calculating the emissivities at the two interfaces, we somewhat arbitrarily choose the depths $z = 0.05\ Z_0$ and $z = 0.95\ Z_0$ as the appropriate depths when calculating the refractive index of the ice. This is an attempt to model the slow variation of the refractive index over a wavelength.

The cosine, μ, of the ice incidence angle Ψ (see Figure 5) is obtained from the generalized Snell's law expression (See Stratton, 1941; p. 502). The variation of μ with depth is not expected to influence significantly the nature of the calculation.

Model calculations are presented in Figures 6 and 7. The particular thin ice parameters specified correspond to the best estimate of experimental conditions of Gloersen and others (1975b); the data are from that paper. The agreement is quite good, though the agreement may be fortuitous since small variations of certain thin ice variables (especially average salinity) affects

the model output noticeably. Clearly, systematic experimental observations over the range of the thin ice parameters (e.g., wavelength, average salinity, average density, ice thickness, surface temperature and incidence angle) are needed.

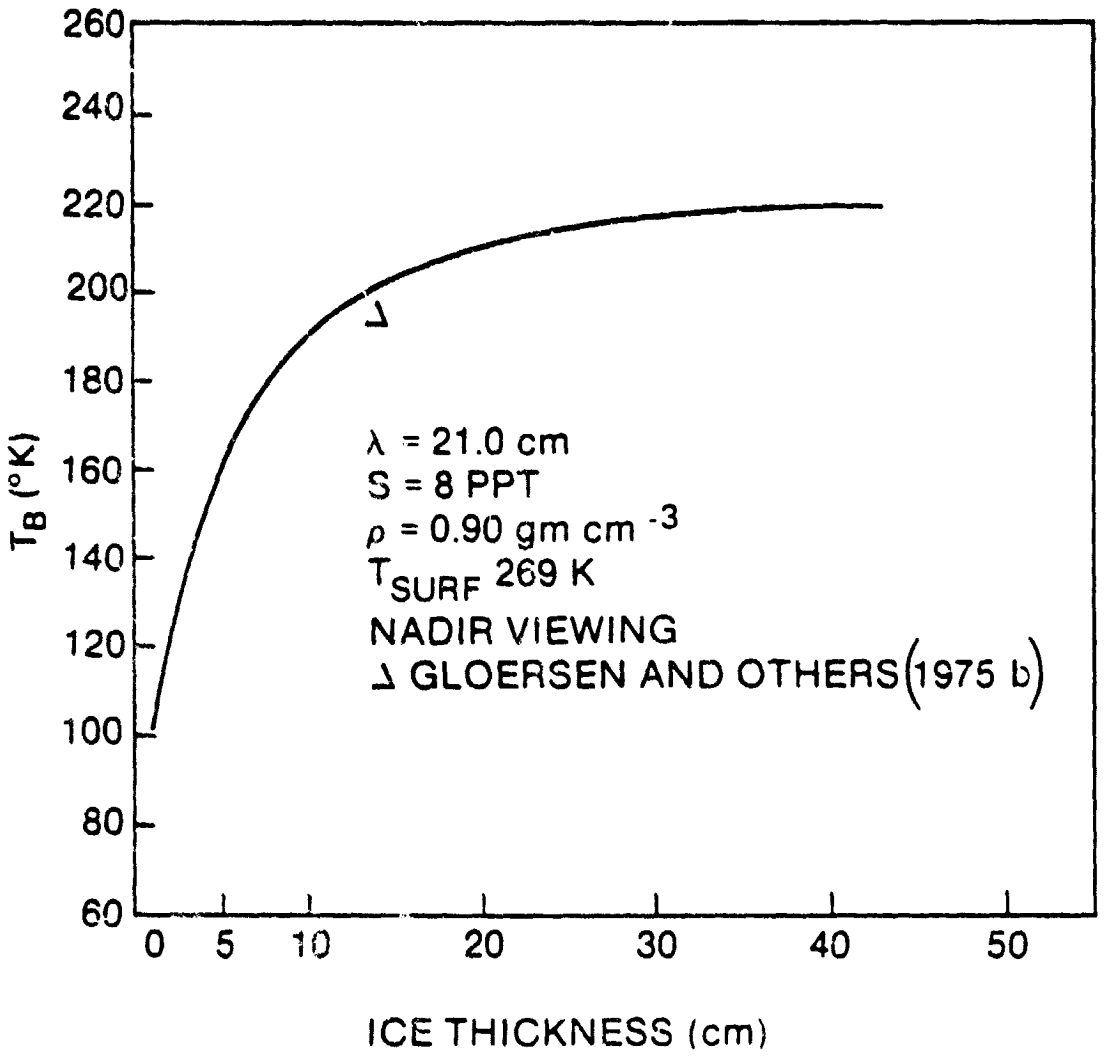

Figure 6. Comparison of model calculations (this paper) and measurements of Gloersen et al., for a surface temperature of 269 K.

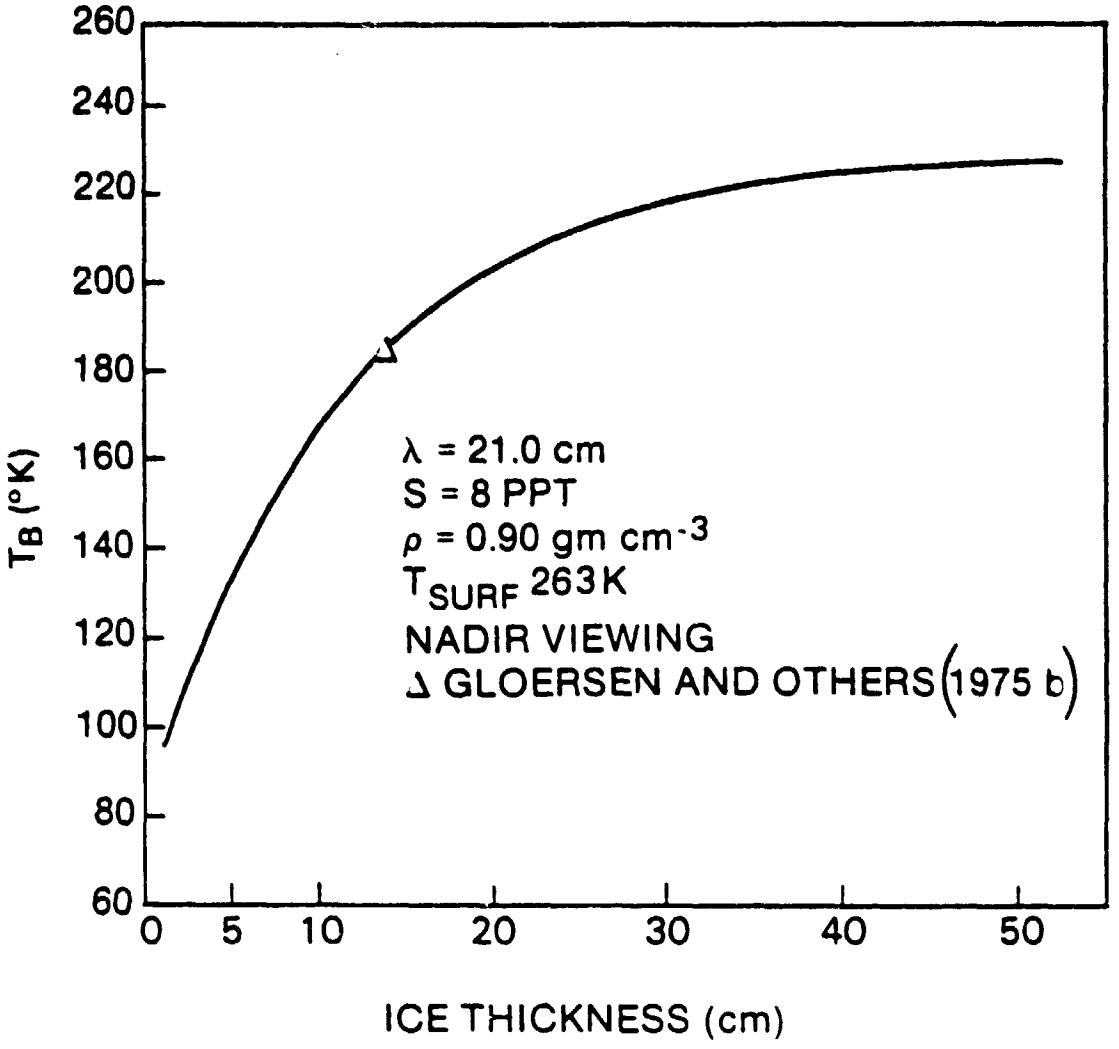

Figure 7. Comparison of model calculations (this paper) and measurements of Gloersen et al. for a surface temperature of 263 K.

4. FIRST YEAR (FY) SEA ICE

As young sea ice ages, it undergoes several morphological changes. These changes are well documented in the sea ice literature (see, for example, Gloersen and others, 1975a; Campbell and others, 1978; Gloersen and others, 1978). The most interesting change in terms of microwave radiometry is the acquisition of a layer of snow. This snow layer differs appreciably in optical properties

from the underlying saline ice. In our treatment of FT ice, scattering contributions to the extinction coefficient were considered negligible relative to absorptive processes. Absorption by snow and scattering by the ice crystals is the dominant contribution to the total extinction coefficient.

Scattering of microwave radiation by snow crystals is tractable upon the imposition of several conditions (Chang and others, 1976). The full Mie (1908) apparatus for the far-field solution of scattering by particles assumes sphericity and scattering incoherence. Though snow crystals are of course not spherical nor are they particularly well separated, these assumptions are not expected to influence the qualitative nature of the results.

Inclusion of scattering effects in the equation of transfer necessitates formulation of the scattering phase function. We will follow Chang and others (1976) and narrow the scope of the problem by assuming azimuthal symmetry in the phase function. and hence obtain nadiral radiances.

We model the refractive index of the snow with a simple mixing formula

$$n'_{snow} = 1.78\,P + 1.00(1 - P) \tag{14}$$

$$n''_{snow} = n''_{pure\ ice}\,P \tag{15}$$

where P is the packing fraction (snow density/ice density), and $n''_{pure\ ice}$ is described by Figure 1. We assume for the purposes of modeling that the snow layer on top of the ice is moderately packed (P = .52). The extinction coefficient τ_e of the snow layer is defined as the sum of absorption and scattering coefficients:

$$\tau_e = \tau_s + \int_0^z \beta(z')\,dz' = \tau_s + \tau_a \tag{16}$$

where the upper limit in τ_a is less than the snow thickness Z_1. Since first-year sea ice is sufficiently thick to attenuate radiation from sea water, we may write the nadir radiance of FY ice as

$$T_B = \epsilon_1 \epsilon_2 T_1 \exp(-\tau_1) + \epsilon_1 T_2 + \epsilon_1 (1 - \epsilon_2) T_3 \exp(-\tau_1) \qquad (17)$$

where ϵ_1 and ϵ_2 are the nadir emissivities at the air/snow and snow/ice interfaces, respectively, and we have neglected any angular redistribution of radiation. As before, the effective temperatures T_1, T_2, and T_3 are weighted averages of the thermodynamic temperatures of the ice and snow layers:

$$T_1 = \int_0^{\tau_{2a}} T_I(z) \exp(-\tau_{2a}'(z)) \, d\tau_{2a}'(z) \qquad (18)$$

$$T_2 = \int_0^{\tau_{1a}} T_s(z) \exp(-\tau_{1a}'(z)) \, d\tau_{1a}'(z) \qquad (19)$$

$$T_3 = \exp(-\tau_{1a}) \int_0^{\tau_{1a}} T_s(z) \exp(\tau_{1a}'(z)) \, d\tau_{1a}'(z) \qquad (20)$$

where $T_I(z)$ and $T_s(z)$ are temperature profiles of the ice and snow layers, respectively, and τ_{2a} and τ_{1a} are the respective extinction coefficients of the ice and snow layers. The temperature profiles are linear at equilibrium; however, the disparate thermal diffusivities of the two media require differing slopes. Application of the flux and continuity boundary conditions yields

$$T_s(z) = T_{surf} + \frac{(T^* - T_{surf})\, z}{z_1} \qquad 0 < z < z_1 \qquad (21)$$

$$T_I(z) = T^* + \frac{(271 - T^*)}{z_2} (z - z_1) \qquad z_1 < z < z_1 + z_2 \qquad (22)$$

$$T^* = \frac{K_1 z_2 T_{surf} + K_2 z \cdot 271}{K_1 z_2 + K_2 z_1} \qquad (23)$$

T^* is the physical temperature at the snow/ice interface. The quantities K and z refer to thermal conductivity and thickness, and the subscripts 1 and 2 to snow and ice layers, respectively. The snow layer is from $z=0$ to $z=z_1$ and the saline ice layer extends from $z=z_1$ to $z=z_2$.

The conductivities are in general multivariate functions of such variables as air flow rate in the snow layer and temperature and salinity changes in the ice layer (Pounder, 1965; p. 140). For a first order calculation, we assume constant values as follows: for snow, $P = 0.52$ and $K_1 = 0.0015$ cal sec^{-1}; cm^{-1} k^{-1} for sea ice, $\rho = 0.91$ gm cm^{-3} and $K_2 = 0.0048$ cal sec^{-1} cm^{-1} k^{-1} (Maykut and Untersteiner, 1971).

External parameters specified *a priori* in the FY ice model are now several in number. Experimental observations yield typical ranges for these parameters. The snow layer thickness z_1, varies from 0-10 cm. FY ice is usually between 40 and 200 cm thick (Ramseier and others, 1975; Gloersen and others, 1975a). Wind-blown snow has a snow crystal radius less than 0.2 mm (Chang and others, 1976).

The number of variables in the FY ice model and the lack of accurate quantification of these variables in the field makes any strict comparison between theory and experiment less than valid. However, for the purposes of discussion, we calculate that with a snow layer thickness of 5 cm, ice layer thickness of 100 cm, a snow crystal radius of 0.2 mm, average salinity of 8 ppt, a snow surface temperature of 258 K, and at 1.55 cm wavelength, FY ice should have a nadir brightness temperature of 252.4 K. Gloersen and others (1973) report 252± 1 K for FY ice with surface temperature of 258 K at 1.55 cm wavelength.

Qualitatively, the primary reason for the high emissivity of FY ice is the mediating refractive index effect of the snow layer, since both ϵ_1 and ϵ_2 are often very close to unity. The insulating character of the snow layer contributes as well, allowing radiation from thermodynamically warm sea ice to escape. Evidence of this behavior was reported by Campbell and others (1978), where removal of snow cover resulted in a drop in brightness of 7°K at 0.8 cm and 12° K at 2.2 cm wavelength.

5. MULTIYEAR SEA ICE

After surviving at least one summer melting period, FY ice undergoes complete recrystallization and desalinization in the freeboard layer (Meeks and others, 1974). The empty brine pockets in the freeboard give rise to volume scattering and lower density. The absence of brine also reduces the value of n'' to nearly that of fresh water ice. Hence the optical properties of the freeboard layer must be considered when modeling MY ice. The submerged portion of MY ice, while less saline than FY ice, is still opaque to microwave radiation. Therefore we may write:

$$T_B = \epsilon_1 \epsilon_2 \epsilon_3 T_3 \exp(-(\tau_2 + \tau_1)) + \epsilon_1 \epsilon_2 T_2 \exp(-\tau_1) + \tag{24}$$

$$\epsilon_1 T_1 + \epsilon_1 \epsilon_2 (1 - \epsilon_3) T_5 \exp(-(\tau_2 + \tau_1)) +$$

$$\epsilon_1 (1 - \epsilon_2) T_4 \exp(-\tau_1)$$

where the emissivities ϵ_1, ϵ_2 and ϵ_3 correspond to the snow/air, desalinated ice/snow, and saline ice/desalinated ice interfaces, respectively, τ_1 and τ_2 are the total opacities of the snow and desalinated ice layers, respectively, and T_1 through T_5 are weighted temperatures as follows:

$$T_1 = \int_0^{\tau_{1a}} T_s(z) \exp(-\tau_{1a}'(z)) \, d(\tau_{1a}'(z)) \tag{25}$$

$$T_2 = \int_0^{\tau_{2a}} T_I(z) \exp(-\tau_{2a}'(z)) \, d(\tau_{2a}'(z)) \tag{26}$$

$$T_3 = \int_0^{\tau_{3a}} T_I(z) \exp(-\tau_{3a}'(z))\, d(\tau_{3a}'(z)) \tag{27}$$

$$T_4 = \exp(-\tau_{1a}) \int_0^{\tau_{1a}} T_s(z) \exp \tau_{1a}'(z)\, d\, \tau_{1a}'(z) \tag{28}$$

$$T_5 = \exp(-\tau_{2a}) \int_0^{\tau_{2a}} T_I(z) \exp \tau_{2a}'(z)\, d\, \tau_{2a}'(z) \tag{29}$$

where τ_3 is total opacity of the saline ice layer and other quantities are as before. The total opacities τ_1 and τ_2 include both absorption and scattering and depend on the complex refractive index of the two layers, the physical dimensions of the scattering centers with the two layers, the microwave wavelength, and the thickness of the two layers. If the extinction coefficient at a given wavelength were the same for all MY ice, it would be possible to infer the thickness of the MY ice from brightness temperatures at several wavelengths. However, no experimental basis exists for this assumption.

Some insight into the problem can be obtained by qualitative analysis of a limited data set obtained from the Nimbus-7 Scanning Multifrequency Microwave Radiometer (SMMR-7) northwest of the Queen Elizabeth Islands in the Arctic Basin, where the pack ice is generally fully consolidated and MY in nature. Surface temperature data during the Nimbus-7 overpass were obtained from a synchronized flight by the NASA CV-990 airborne laboratory (Gloersen and others, unpublished data). We simplify equations (24) through (29) as follows. We assume (1) that the surface temperature inferred from the infrared sensor onboard the CV-990 can be used tc determine the effective radiating temperature of the MY pack, (2) the snow layer can be neglected, and (3) the freeboard layer is uniform in its optical properties and has negiigible absorption.

With these assumptions, $\epsilon_1 = \epsilon_2 = \epsilon_3 = 1, \tau_1 = \tau_{2a} = 0$, and $\tau_3 >> 1$, where 1, 2, and 3 cor-

respond to th: snow, freeboard, and submarine layers of the ice, respectively. Hence, in equations (25) - (29), $T_1 = T_2 = T_4 = T_5 = 0$, and equation (24) reduces to

$$T_B = ((271 - T_{surf})/8 + T_{surf}) \exp(-\tau_2) = \epsilon ((271 - T_{surf})/8 + T_{surf}) \qquad (30)$$

In equation (30), the effective radiating temperature corresponds to the physical temperature of the ice near sea level. The emissivity of MY ice as observed from SMMR-7 is plotted in Figure 8. The wavelength dependence of the extinction coefficient is not inverse fourth power (Figure 9,) as would be expected if the scattering were Rayleigh in nature.

6. ATMOSPHERE EFFECTS

Data obtained from spacecraft contain effects originating in the opacity and physical temperature profile of the atmosphere. For sea ice observations, however, atmospheric contributions are generally negligible due to the low humidity and near-absence of liquid water droplets in the polar troposphere. Cloud cover is usually low-altitude stratus and occasional high-altitude cirrus, both essentially transparent at microwave wavelengths. Clouds principally affect the microwave radiance from sea ice by changing the radiative balance at the air/ice interface and thus altering the surface temperatures. However, these conditions do no necessarily obtain near the sea ice boundaries, where rainfall occurs.

7. CONCLUSIONS

We have presented a model for the complex refractive index of sea ice, an important parameter in the understanding of microwave emission from sea ice. Utilizing this model as a basis, the microwave properties of first-year thin, first-year with snow cover, and multiyear sea ice have been investigated, employing empirically derived knowledge of the vertical structure of the three types of sea ice. A complete understanding of the microphysics of microwave emission from sea ice awaits more extensive measurements in the field and from space.

EMISSIVITIES BASED ON NIMBUS-7 SMMR OBSERVATIONS

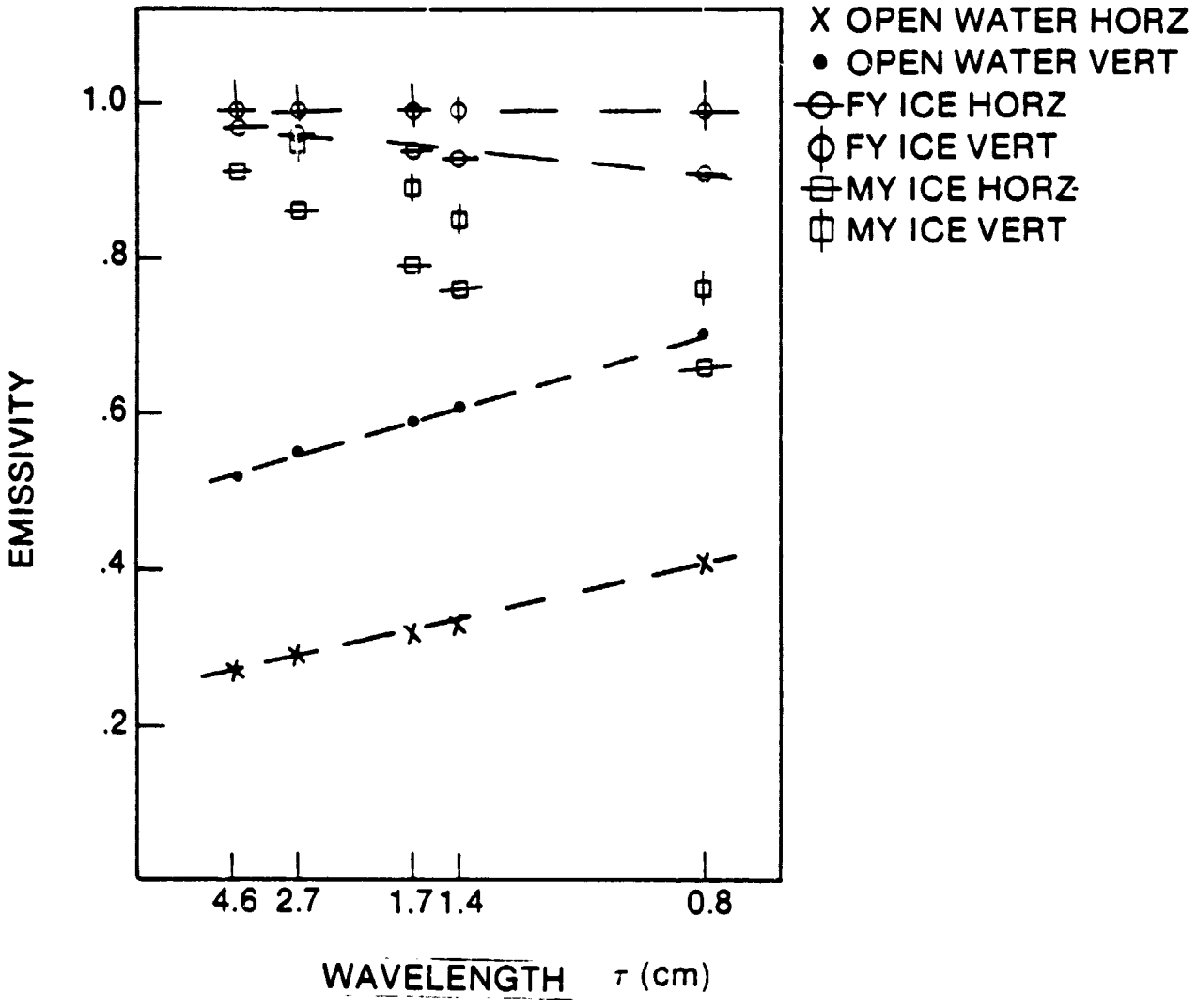

Figure 8. Observed microwave emissivity as a function of wavelength (Gloersen & Cavalieri, to be published).

REFERENCES

1. Assur, A., 1958: Composition of sea ice and its tensile strength in Arctic Sea Ice, NAS-NRC Publ. No. 598, p. 106-138.
2. Basharinov, A. Ye., A. S. Gurvich, and S. T. Yegorov, 1974: Radio emission from the earth as a planet, Moscow, Nauka Press.
3. Campbell, W. J., J. Wayenberg, J. B. Ramseyer, R. O. Ramseier, M. R. Vant, R. Weaver, A. Redmond, L. Arsenault, P. Gloersen, H. J. Zwally, T. T. Wilheit, T. C. Chang, D. Hall, L. Gray, D. C. Meeks, M. L. Bryan, F. T. Barath, C. Elachi, R. Leberl, and T. Farr, 1978: Microwave remote sensing of sea ice in the AIDJEX main experiment, Bdry. Layer Met. *13*, p. 309-337.
4. Chandrasekhar, S., 1960: Radiative transfer, New York, Dover Publications, Inc.
5. Chang, T. C., P. Gloersen, T. Schmugge, T. T. Wilheit, and H. J. Zwally, 1976: Microwave emission from snow and glacier ice, J. Glaciol. *16*, 74, p. 23-39.
6. Frankenstein, G., and R. Garner, 1967: Equations for determining the brine volume of sea ice from -5° to -22°, J. Glaciol. *6*, p. 943.
7. Gloersen, P., W. Nordberg, T. J. Schmugge, and T. T. Wilheit, 1973: Microwave signatures of first-year and multiyear sea ice, J. Geophys. Res., *78*, 18, p. 3564-3.
8. Gloersen, P., R. Ramseier, W. J. Campbell, T. C. Chang, and T. T. Wilheit, 1975a: Variation of ice morphology of selected mesoscale test areas during the Bering Sea Experiment, Proceedings of the Final Symposium on the Results of the Joint USSR/USA Bering Sea Experiment, Leningrad, Gidometeoizdat, p. 196-218.
9. Gloersen, P., R. Ramseier, W. J. Campbell, P. Kuhn, and W. J. Webster, Jr., 1975b: Ice thickness distribution as inferred from infrared and microwave remote sensing during the Bering Sea Experiment. (same as above (8.)), p. 282-293.
10. Gloersen, P., H. J. Zwally, A. T. C. Chang, D. K. Hall, W. J. Campbell, and R. O. Ramseier, 1978: Time dependence of sea ice concentration and multiyear ice fraction in the Arctic Basin, Bdry. Layer Met. *13*, p. 339-359.

11. Gunn, L. L. S., and T. U. R. East (1954), The microwave properties of precipitation particles, Quart. J. Roy. Meteorol. Soc., *80*, 522-554.

12. Hallikainen, M., 1973: Analysis of dielectric properties and noise temperature 1973 European Microwave Conference, No. 2, C. 15.3, Brussels.

13. Ho, W., and W. F. Hall, 1973: Measurements of the dielectric properties of sea water and NaCl solutions at 2.65 GHz., J. Geophys. Res. *78*, p. 6301-6315.

14. Hoekstra, P., and P. Cappillino, 1971: Dielectric properties of sea and sodium chloride ice at UHF and microwave frequencies, J. Geophys. Res. *76*, p. 4922-4931.

15. Hoekstra, P., and T. E. Osterkamp, and W. F. Weeks, 1965: Migration of liquid inclusions in single ice crystals, J. Geophys. Res. *70*, p. 5035-5041.

16. Jackson, J. D., 1975: Classical electrodynamics. New York, John Wiley and Sons, Inc.

17. Klein, L. A., and C. T. Swift, 1977: An improved model for the dielectric constant of sea water at microwave frequencies, IEEE Trans. Ant. Prop. *AP-25*, 1, p. 104-111.

18. Landau, L. D., and E. M. Lifshitz, 1975: Electrodynamics of continuous media, Oxford, Pergamon Press.

19. Lane, J. A., and J. A. Saxton, 1952a: Dielectric dispersion in pure polar liquids at very high radio-frequencies. I. Measurements on water, methyl and ethyl alcohols. Proc. Roy. Soc. *A213*, p. 401-408.

20. Lane, J. A., and J. A. Saxton. 1952b: Dielectric dispersion in pure polar liquids at very high radio-frequencies. III. The effect of electrolytes in solution. Proc. Roy. Soc., *A214*, p. 531-545.

21. Maykut, G., and N. Untersteiner, 1971: Some results from a time-dependent thermodynamic model of sea ice, J. Geophys. Res. *76*, p. 1550-1575.

22. Meeks, D. C., R. O. Ramseier, and W. J. Campbell, 1974: A study of sea ice-AIDJEX 1972, Proceedings of the Ninth International Symposium on Remote Sensing of Environment, Ann Arbor, Michigan, ERIM, p. 301-322.

23. Mie, G., 1908: Beitrage zur Optik truber Medien, speziell kolloidaler Metallogsungen, Ann. Phys. Vierte Folge, Bd. 25, HH. 3, p. 337-445.

24. Poe, G., A. Stogryn, and A. T. Edgerton, 1972: A study of the microwave emission characteristics of sea ice, Final Technical Report 1749R-2, Contract No. 2-35340, Azusa, California, Aerojet-Electrosystems Co.

25. Pounder, R. R., 1965: The physics of ice, Oxford, Pergamon Press.

26. Ramseier, R. O., P. Gloersen, W. J. Campbell, and T. C. Chang, 1975: Mesoscale description for the principal Bering Sea Experiment, (same as 8), p. 234-269.

27. Stogryn, A., 1971: Equations for calculating the dielectric constant of saline water, IEEE Trans Micro. Theory and Techniques, *MTT-19*, p. 733-736.

28. Stratton, J. A., 1941: Electromagnetic theory, New York, McGraw-Hill Book Co., Inc.

29. Tiuri, M., Hallikainen, M., and A. Laaperi, 1978: Radiometer studies of low-salinity sea ice, Bdry. Layer Met. *13*, p. 361-371.

30. Untersteiner, N., 1968: Natural desalination and equilibrium salinity profile of perennial sea ice, J. Geophys. Res. *73*, p. 1251-1257.

31. Vant, M. R., 1976: A combined empirical and theoretical study of the dielectric properties of sea ice over the frequency ranges 100 MHz to 40 GHz. Technical Report, Ottawa, Canada, Carleton University/Environment Canada.

32. Vant, M. R., R. B. Gray, R. O. Ramseier, and V. Makios, 1974: Dielectric properties of fresh and sea ice at 10 and 35 GHz, J. Appl. Phys. *45*, p. 4712-4717.

FIGURE CAPTIONS

Figure 1. Real and imaginary parts of the complex index of refraction for pure ice.

Figure 2. Ratio of the brine volume fraction to its salinity as a function of the ice temperature.

Figure 3. Comparison of the experimental values for the real part of the complex index of refraction for sea ice, obtained from data of Vant et al., and predicted values from the model presented here.

Figure 4. Comparison of the experimental values for the imaginary part of the complex index of refraction for sea ice, obtained from data of Vant et al., and predicted values from the model presented here.

Figure 5. Model schematic for thin sea ice.

Figure 6. Comparison of model calculations (this paper) and measurements of Gloersen et al., for a surface temperature of 269 K.

Figure 7. Comparison of model calculations (this paper) and measurements of Gloersen et al. for a surface temperature of 263 K.

Figure 8. Observed microwave emissivity as a function of wavelength (Gloersen & Cavalieri, to be published).